J Nanopart Res (2010) 12:2111–2124
DOI 10.1007/s11051-009-9770-3

RESEARCH PAPER

Synthesis of thiol-functionalized MCM-41 mesoporous silicas and its application in Cu(II), Pb(II), Ag(I), and Cr(III) removal

Shengju Wu · Fengting Li · Ran Xu · Shihui Wei · Guangtao Li

Received: 29 May 2009 / Accepted: 21 September 2009 / Published online: 7 October 2009

Abstract Thiol-functionalized MCM-41 mesoporous silicas were synthesized via evaporation-induced self-assembly. The mesoporous silicas obtained were characterized by X-ray diffraction (XRD), nitrogen adsorption–desorption analysis, Fourier transform infrared spectroscopy (FTIR), elemental analysis (EA), transmission electron microscopy (TEM), and scanning electron microscopy (SEM). The products were used as adsorbents to remove heavy metal ions from water. The mesoporous silicas (adsorbent A) with high pore diameter (centered at 5.27 nm) exhibited the largest adsorption capacity, with a BET surface area of 421.9 $m^2\ g^{-1}$ and pore volume of 0.556 $cm^3\ g^{-1}$. Different anions influenced the adsorption of Cu(II) in the order $NO_3^- < OAc^- < SO_4^{2-} < CO_3^{2-} < Cit^- < Cl^-$. Analysis of adsorption isotherms showed that Cu^{2+}, Pb^{2+}, Ag^+, and Cr^{3+} adsorption fit the Redlich–Peterson nonlinear model. The mesoporous silicas synthesized in the work can be used as adsorbents to remove heavy metal ions from water effectively. The removal rate was high, and the adsorbent could be regenerated by acid treatment without changing its properties.

Keywords Mesoporous silicas · Adsorbent · Heavy metal · Regeneration · Adsorption · Environmental remediation · EHS

S. Wu · F. Li (✉) · R. Xu · S. Wei
State Key Laboratory of Pollution Control and Resource Reuse, College of Environmental Science & Engineering, Tongji University, 20092 Shanghai, China
e-mail: fengting@tongji.edu.cn

G. Li
Department of Chemistry, Tsinghua University, 100084 Beijing, China

Introduction

A large variety of heavy metals are discharged into the environment, causing serious environmental pollution even at low concentrations. However, many of them (e.g., silver, lead and copper) are precious metals with extensive applications, which could be recycled and reused. Adsorption technology is one of the most popular methods to control and concentrate these heavy metals (Mureseanu et al. 2008; Yang et al. 2008; Xue and Li 2008). Activated carbon and a number of low-cost adsorbents such as rice husks, boehmite, montmorillonite, and low-cost adsorbent materials from paper industrial waste materials have been used to remove heavy metal ions (Correa and Becerril 2009; Kang et al. 2004a, b; Bhattacharyya and Gupta 2007; Kubilay et al. 2007). Nevertheless, most of these materials suffer from inherent problems such as low removal capacity, low selectivity, long equilibrium time, or mechanical and thermal instability. In recent years, the preparation of silica-based adsorbents has generated considerable interest due to their unique large specific surface area, regular pore structure and

easily modified surface properties (Mureseanu et al. 2008; Yang et al. 2008; Xue and Li 2008).

Modified mesoporous silicas are promising adsorbents with high adsorption capacity for heavy metals. The adsorption mechanism for the removal of toxic heavy metal ions in an aqueous solution is either by electrostatic interaction (ionic interaction between positively charged metal ions and negatively charged matrices) or by chelation (donation of the lone-pair electrons of the matrices to metal ions to form coordinate bonds) (Cestari et al. 2009; Quintanilla et al. 2006). Although the cost for mesoporous adsorbents per unit is relatively high, some of them can be economically regenerated, while maintaining their great adsorption capacity for heavy metals after multiple reuses (Lu and Yan 2004; Burleigh et al. 2001; Sayari et al. 2005). Hydrothermal synthesis is a common method to prepare mesoporous materials (Wei et al. 2005). This method uses organic and inorganic reactants combined in water, which easily results in rapid hydrolysis of organosilane and reduces the cross-linking of the organosilane. At the same time, the silica framework can be modified easily by functional groups in the use of this method.

Evaporation-induced self-assembly (EISA) procedure is based on sol–gel chemistry and is mainly used for preparation of mesoporous films (Naik et al. 2006). The mesoporous silicas are usually modified in a one or two-step procedure. In both methods, organic functional groups are attached to the framework. For example, the removal efficiency of Cu^{2+}, Cd^{2+}, Hg^{2+}, increases remarkably after mesoporous silicas such as SBA-15, MCM-41, HMS have been modified with $–NH_2$, –SH, and $–SO_3H$, respectively (Wu et al. 2007; Zhang et al. 2007a, b). The two-step procedure (post-synthesis treatment) is to graft organic groups onto the preformed mesopore channel surface (Yang et al. 2005; Kang et al. 2004a, b), which can easily lead to morphological damage and a low ratio of modified functional groups. In comparison, the one-step procedure directly incorporates organic groups into the silica frame by condensation, which results in an uniform distribution of functional groups inside the mesopore channels but leads to smaller pore sizes (Yang et al. 2004; Li et al. 2007). The one-step procedure is favorable for the production of adsorbents (Zhang et al. 2007a, b). Among the mesoporous silicas, MCM-41 shows high removal rate, high selectivity, short equilibrium time, and good mechanical stability in the adsorption of heavy metal ions from aqueous solution (Yang et al. 2008; Mangrulkar et al. 2008). However, it is the first time to report thiol-functionalized MCM-41-based mesoporous silicas. Studies of the effect of different anions on heavy metal ion removal by mesoporous silicas are rare.

This work explores the preparation of new thiol-functionalized MCM-41-based mesoporous silicas and their application for Cu(II), Pb(II), Ag(I), and Cr(III) removal. A new hybrid material was synthesized and characterized: MCM-41 mesoporous silica modified with 3-mercaptopropyltrimthoxysilane (MPTMS). The applicability of this material for removal of Cu^{2+}, Cr^{3+}, Pb^{2+}, and Ag^{+} from water solutions was studied. The influence of anions on the adsorption of Cu(II) was investigated. First, the obtained adsorption isotherm provided useful information for the mechanism of Cu^{2+}, Cr^{3+}, Pb^{2+}, and Ag^{+} adsorption by the functionalized mesoporous silica. Second, the equilibrium adsorption capacity provides a measurement of the total amount of material that can be adsorbed by the mesoporous material under specific temperature and concentration conditions.

Experimental

Reagents and materials

MPTMS (3-mercaptopropyltrimethoxysilane, 99%) was purchased from Aldrich. Tetraethyl orthosilicate (TEOS), cetyltrimethyl ammonium bromide (CTAB), absolute ethylalcohol, and tetramethylammonium hydroxide (TMAOH, 25 wt%) were provided by Sinopharm Chemical Reagent Company. All the above materials were used without further purification. Nitrates of copper, lead, chrome, and silver were used to prepare the metal ion solutions. No further pH adjustment of these solutions was made. Deionized water was used throughout this work.

Methods

Synthesis of functionalized mesoporous silica

A typical synthetic procedure used TEOS and MPTMS in relative molar ratios of 4:1. In a typical synthesis, 2.19 g CTAB was dissolved in 35 g dry ethanol and vigorously stirred for 2 h. Separately, 3.64 g 25%

TMAOH, 25 g dry ethanol, and 1.54 g MPTMS were mixed and stirred for 2 h. Then the above solutions were mixed and 6.64 g TEOS was slowly dripped into the mixture. After addition of TEOS was complete, the mixture was stirred for 1 h. The final product was transferred into a Petri dish for solvent evaporation at room temperature. The residue was aged in deionized water at 90°C for 3 days. After recovery by filtration, the solid product was washed with refluxing mixture of ethanol/HCl (molar ratio = 70:1) for 1 day at 70°C to extract the surfactant template. Then it was filtered, stirred in 1 mol L^{-1} $NaHCO_3$ aqueous solution for 8 h and washed with deionized water for neutralization. Finally, it was dried under vacuum at 60°C for 1 day to obtain the adsorbent powder. The synthesis route is shown in Fig. 1. The resulting functionalized MCM-41 sample is denoted adsorbent A.

The syntheses of adsorbents B, C, and O were similar to the one described above. The quantities of CTAB, HCl, TMAOH, and ethanol are the same with adsorbent A. The weights of TEOS MPTMS and the molar ratio of TEOS/MPTMS are shown in Table 1.

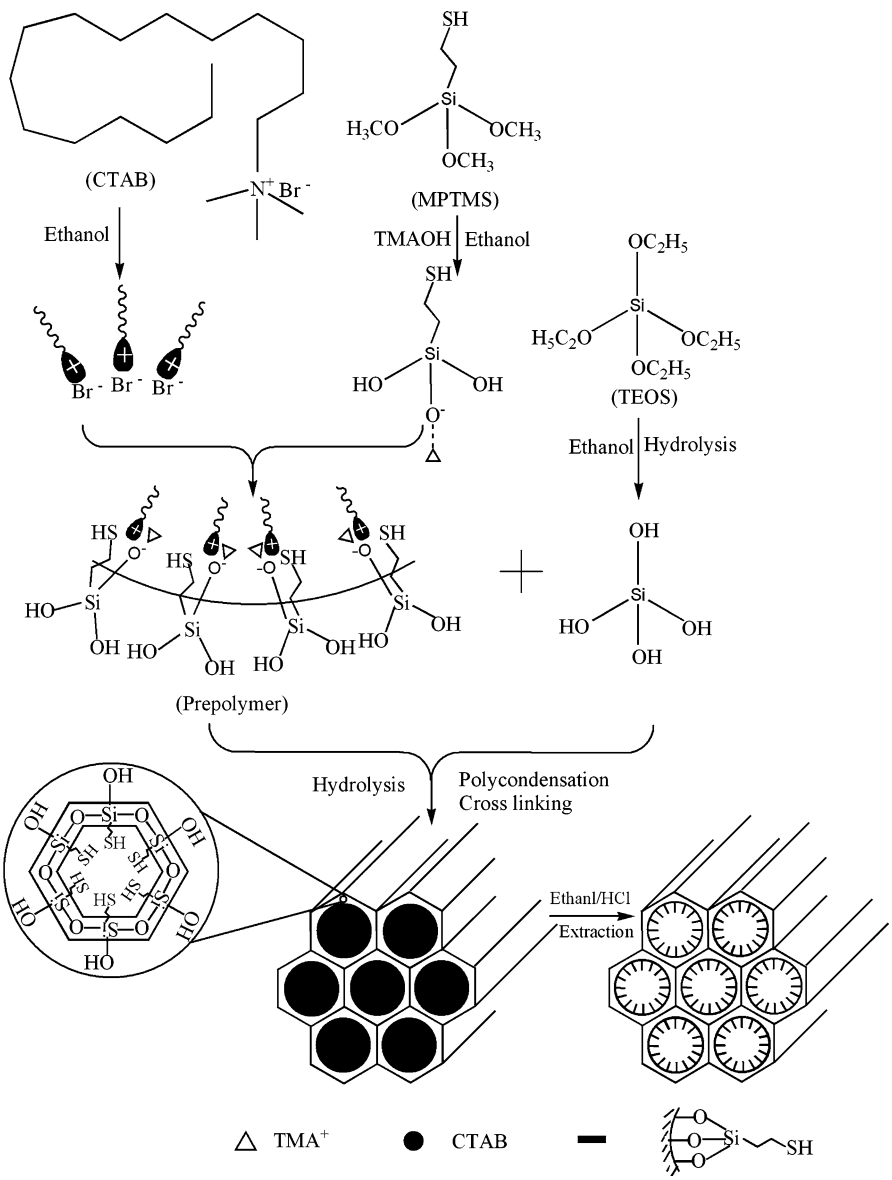

Fig. 1 The synthesis route to mesoporous silicas with mercapto groups

Table 1 Amount of raw materials used in the syntheses of the MCM-41 adsorbents

Samples	TEOS/MPTMS (molar ratio)	MPTMS	TEOS
O	–	0	8.13
A	4.0:1	1.54	6.64
B	3.5:1	1.76	6.49
C	3.0:1	1.97	6.25

Characterization of mesoporous adsorbents

The adsorbents were characterized by common analytical techniques. X-ray diffraction (XRD) patterns of the MCM-41 and SH-MCM-41 mesoporous silicas were obtained on a D8 Advance Diffractometer (40 kV, 100 mA, Cu Kα, 2 h = 0.4°–10°). Nitrogen adsorption measurements were carried out at 77 K using a Coulter Omnisorp 100 gas analyzer. The specific surface area was calculated by employing the Brunauer–Emmett–Teller (BET) method in the range of relative pressure from 0.05 to 0.2. The pore volume and pore size distributions were calculated using the Barrett–Joyner–Halenda (BJH) model on the adsorption branch. FTIR spectra were obtained on a Spectrum 2000 FTIR spectrometer (Perkin-Elmer) by the KBr pellet method. The sulfur content was determined by an Elemental Analyser (Vario EL, CHNS). Transmission electron microscope (TEM) imaging was performed using a JEM-2011 electron microscope operated at 200 kV. SEM images were obtained with a field emission XL-30 ESEM microscope operating at 30 kV. The concentrations of Cu^{2+}, Pb^{2+}, Pb^{2+}, and Ag^{+} remaining in the solutions were analyzed by an Inductively Coupled Plasma Spectrometer (ICP, Optima 2100 DV, America) after appropriate dilution. The pH values were measured by a pH-meter (PHS-3C, China).

The adsorption isotherm of the functionalized silica

To measure the adsorption isotherms, approximately 100 mg of adsorbent A and 100 ml of Cu^{2+}, Pb^{2+}, Ag^{+}, or Cr^{3+} solution with different concentrations (0.2, 0.4, 0.6, 0.8, 1.0, 1.5, 2.0, 3.0 mmol L^{-1}) were added to a 250-ml conical flask. The initial pH value was adjusted to 5 with dilute nitric acid and sodium hydroxide solution. After shaking (200 r min^{-1}) for 60 min at different temperature (293, 303, 313 K), the suspension was separated with a 0.45 μm Uniflo filter. The filtrate was analyzed for Cu^{2+}, Pb^{2+}, Ag^{+}, and Cr^{3+} by ICP/OES spectroscopy.

Effect of pH on adsorption

The effect of pH on the adsorption was determined in experiments analogous to the adsorption isotherm experiments using approximately 100 mg of adsorbent A and 100 ml of 1.0 mmol L^{-1} Cu^{2+}, Pb^{2+}, Ag^{+}, or Cr^{3+} solution. Dilute nitric acid and sodium hydroxide solutions were used to adjust the initial pH value to 2, 3, 4, 5, 6, or 7. After shaking (200 r min^{-1}) for 60 min at 313 K, the suspension was separated with a 0.45 μm Uniflo filter. The filtrate was analyzed for Cu^{2+}, Pb^{2+}, Ag^{+}, and Cr^{3+} by ICP/OES spectroscopy and the final pH value of the filtrate was determined.

Competitive adsorption on the functionalized mesoporous silica

Mixed solutions containing two of the cations Cu^{2+}, Pb^{2+}, Ag^{+}, or Cr^{3+} were prepared to observe the effect of competing cations on metal ion adsorption by the different adsorbents. The ions were tested in the following six combinations: $Cu^{2+} + Ag^{+}$, $Cu^{2+} + Pb^{2+}$, $Cu^{2+} + Cr^{3+}$, $Ag^{+} + Pb^{2+}$, $Ag^{+} + Cr^{3+}$ and $Pb^{2+} + Cr^{3+}$. The concentration of each heavy metal in the mixed solutions was 1.0 mmol L^{-1}. In each conical flask, approximately 100 mg of adsorbent A and 100 ml of mixed solution were added and dilute nitric acid and sodium hydroxide solutions were used to adjust the initial pH to 5. After shaking (200 r min^{-1}) for 60 min at 313 K, the suspension was separated with a 0.45 μm Uniflo filter. The filtrate was analyzed for Cu^{2+}, Pb^{2+}, Ag^{+}, and Cr^{3+} by ICP/OES spectroscopy.

Effect of anions

To observe the effect of anions on Cu^{2+} adsorption by the adsorbents, about 50 ml of 0.1 mol L^{-1} NaCl, $NaNO_3$, Na_2SO_4, Na_2CO_3, NaOAc, or NaCit solution was added to a flask containing 100 mg of adsorbent, then 50 ml 2 mmol L^{-1} Cu^{2+} solution was added and the pH adjusted to 5. After the shaking for 60 min at 303 K, the suspension was filtered through a 0.45 μm

Uniflo filter. The filtrate Cu^{2+} concentration was determined by ICP/OES spectroscopy. A 1 mmol L^{-1} solution of Cu^{2+} in deionized water was used as blank.

Regeneration of adsorbent A

We determined how effectively adsorbent A could be regenerated after adsorption of Cu^{2+}, Pb^{2+}, Ag^{+}, and Cr^{3+} as follows. About 100 ml of mixed solution was added to a 250 ml conical flask containing 100 mg of adsorbent A. The concentration of Cu^{2+}, Pb^{2+}, Ag^{+}, and Cr^{3+} in the mixed solutions was 1.0 mmol L^{-1}. After the shaking for 60 min at 303 K, the suspension was separated with a 0.45 μm Uniflo filter. The filtrate Cu^{2+}, Pb^{2+}, Ag^{+}, and Cr^{3+} concentration was measured with ICP/OES spectroscopy. The silver-loaded adsorbent was then stirred in 100 ml 1 mol L^{-1} HNO_3 solution for 6 h at room temperature to strip the Cu^{2+}, Pb^{2+}, Ag^{+}, and Cr^{3+} ions from the adsorbent. Then the suspension was filtered and the residue was added to 1 mol L^{-1} $NaHCO_3$ solution and stirred for 24 h at room temperature. After filtration and washing, the sample was neutralized to pH 7. The cleaned sample was then dried in a vacuum oven at 60°C. The adsorption–desorption cycle was repeated five times. The sulfur content was measured after each extraction cycle. After six regeneration cycles, the adsorbent was dissolved in 100 ml dilute nitric acid and the solution was allowed to stand for 3 h. The solution was then diluted to 500 ml to measure the Cu^{2+}, Pb^{2+}, Ag^{+}, and Cr^{3+} concentration using ICP/OES spectroscopy.

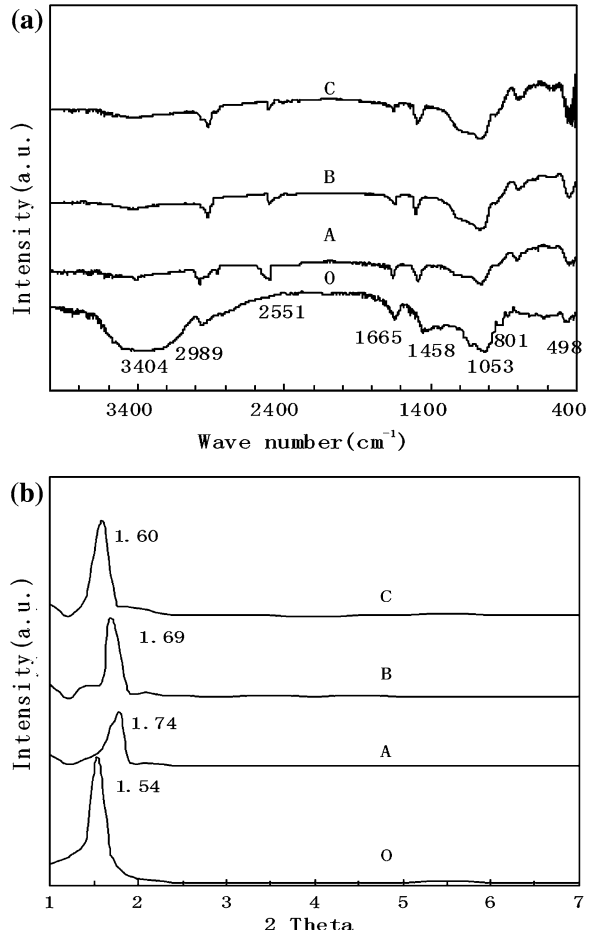

Fig. 2 **a** FTIR spectra pattern of mesoporous adsorbents. **b** XRD patterns of mesoporous absorbents. Adsorbent O is non-functionalized mesoporous material. Adsorbents A–C are functionalized materials. Adsorbent A (TEOS/MPTMS = 4.0:1), adsorbent B (TEOS/MPTMS = 3.5:1), adsorbent C (TEOS/MPTMS = 3.0:1)

Results and discussion

Characterization of mesoporous adsorbents

The adsorbents were examined by FTIR to characterize the modification with –SH. The FTIR patterns of all four adsorbents showed similar locations and appearances of the major bands (Fig. 2a). The features around 801 and 1,053 cm^{-1} are assigned to the Si–O–Si stretching vibrations. The vibrations of Si–OH appeared around 1,653 and 3,404 cm^{-1} (Yang et al. 2006). The bands at 2,989 and 1,458 cm^{-1} resulted from –CH vibrations. The spectra of adsorbents A–C showed characteristic bands for mercapto groups around 2,551 cm^{-1} (Xue and Li 2008; Liu et al. 2009), so we conclude that mercapto groups have been successfully grafted onto the mesoporous silica skeleton by hydrolysis poly condensation. The modification ratio of mercapto groups on the surface of adsorbent A was the highest among adsorbents A–C. The XRD patterns for mesoporous adsorbents are shown in Fig. 2b. The X-ray patterns suggest that the synthesized materials retained the mesoporous structure without significant impairment after modification. Adsorbent A displayed the highest 2θ value (1.74°), which indicates that the modification ratio of mercapto groups on the surface of adsorbent A was the highest.

In Fig. 3a, the pore size distributions of adsorbent O and adsorbents A–C are shown. The pore size of the mesoporous silica decreased after modification because of the organic functional groups in the mesopore channels (Bendahou et al. 2008). The nitrogen adsorption–desorption isotherms for the mesoporous silicas are shown in Fig. 3b. After addition of the S–H groups, the inflection position shifted slightly toward lower relative pressures and the volume of nitrogen adsorbed decreased, which was also indicative of a reduction in pore size (Bendahou et al. 2008). The inflection position of adsorbent A displayed the lowest relative pressure (0.4) indicating that the modification ratio of mercapto groups on the surface of adsorbent A was the highest.

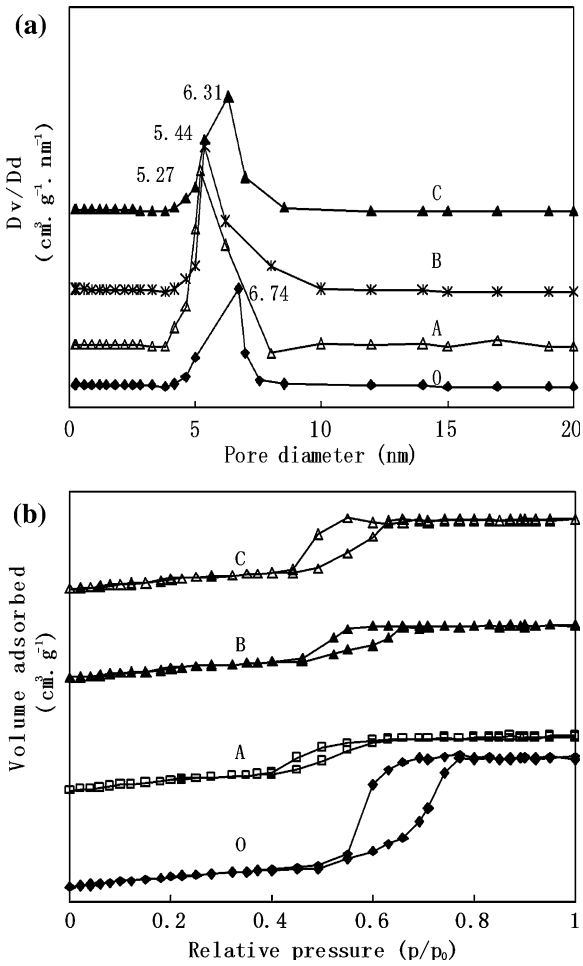

Fig. 3 **a** Pore size distribution of the mesoporous absorbents. **b** Nitrogen adsorption–desorption isotherms of mesoporous absorbent

The structural properties of pure and adsorbent performance functionalized samples were shown in Table 2. The surface area, pore volume and pore size of the functionalized adsorbents A–C were all lower than the non-functionalized sample (O).

The elemental analysis (EA) data in Table 2 indicate that the modification ratio of mercapto groups on the surface of adsorbent A was the highest. Figure 4a and b shows SEM images of adsorbent A, which is a highly crystalline material with clearly visible cubic crystals. The TEM images of the samples in Fig. 4c and d shows a highly ordered body-centered mesostructure, observed along the (100) direction.

Adsorption isotherm of functionalized silica

Langmuir (Eq. 5), Freundlich (Eq. 6) and Redlish–Peterson equations (Eq. 7) were used to analyze the experimental adsorption isotherms in Fig. 5.

$$q_e = \frac{QbC_e}{1 + bC_e} \tag{5}$$

$$q_e = KC_e^{\frac{1}{n}} \tag{6}$$

$$q_e = \frac{PC_e}{1 + \alpha C_e^{\beta}} \tag{7}$$

In all three equations, q_e is the sorption amount per unit of adsorbent (mmol g^{-1}) and C_e is the equilibrium concentration (mmol L^{-1}) of heavy metal ions. In Eq. 5, Q represents the saturation capacity of the adsorbent (mmol g^{-1}) and b is the Langmuir isotherm constant (L/mmol). In the Freundlich model (Eq. 6), K and n are constants specific to the adsorbent. In Eq. 7, P is the Redlich–Peterson isotherm constant (L/mmol), α is the Redlich–Peterson isotherm constant (L/mmol), and β is the exponent, which lies between 0 and 1. If $\beta = 1$, the Redlich–Peterson equation becomes a Langmuir type form.

The isotherms of all three models for Cu^{2+}, Pb^{2+}, Ag^{+}, Cr^{3+} adsorption on adsorbent A are displayed in Fig. 5, and the corresponding parameters are listed in Tables 3, 4 and 5. The adsorption of Cu^{2+}, Pb^{2+}, Ag^{+}, Cr^{3+} ions increased rapidly in the initial phase and then the increasing trend decreased as the initial concentration increased. The initial increase might be due to the high surface area, many available binding sites (such as mercapto groups, primary and secondary hydroxyl groups), and inter and intra pores in the adsorbent (Mureseanu et al. 2008; Yang et al. 2008;

Table 2 Physical properties of the mesoporous silicas

Sample	Surface area ($m^2\ g^{-1}$)	Pore volume ($cm^3\ g^{-1}$)	Pore size (nm)	Elemental composition (wt%)					
				C	H	S	$Si_{organic}$	$Si_{inorganic}$	O
O[a]	587.9	0.927	6.74	5.53	3.14	0	0	38.56	54.37
A[b]	421.9	0.556	5.27	9.82	3.06	8.42	8.25	25.17	44.28
B[c]	442.3	0.602	5.44	9.78	2.97	8.36	8.21	25.83	45.34
C[d]	534.1	0.843	6.31	8.43	2.72	8.04	7.99	28.96	47.97

[a] Adsorbent O is non-functionalized mesoporous material

[b] The molar ratio of TEOS/MPTMS in adsorbent A is 4.0:1

[c] The molar ratio of TEOS/MPTMS in adsorbent A is 3.5:1

[d] The molar ratio of TEOS/MPTMS in adsorbent A is 3.0:1

[e] $\mathrm{Si}\% = \frac{M_{\mathrm{Si}}(1-\mathrm{C}\%-\mathrm{H}\%-\mathrm{S}\%)}{M_{\mathrm{Si}}+2M_{\mathrm{O}}}$ (1)

$Q_{\mathrm{S}} = Q_{\mathrm{Si_{organic}}} = \frac{1000\times \mathrm{S}\%}{M_{\mathrm{S}}}$ (2)

$\mathrm{Si_{organic}}\% = \frac{Q_{\mathrm{Si_{organic}}}\times M_{\mathrm{Si}}}{1000}\times 100\%$ (3)

$\mathrm{Si_{inorganic}}\% = \mathrm{Si}\% - \mathrm{Si_{organic}}\%$ (4)

In above four equations, C%, H%, S%, Si%, $Si_{organic}$%, and $Si_{inorganic}$% represent elemental composition (wt%) of C, H, S, Si, $Si_{organic}$ and $Si_{inorganic}$, respectively, M_{Si} and M_S are molar mass (g/mol)of Si and S, Q_S and $Q_{Si_{organic}}$ represent molar quantum (mmol/g) of S and $Si_{inorganic}$. The premises of calculation are: Si and O in the mesoporous silicon skeleton is a form of silicon–oxygen tetrahedron. The molar ratio of silicon:oxygen is 1:2, namely. In addition, the synthesis reaction conditions are mild, the fracture of Si–$(CH_2)_3$–SH does not occur

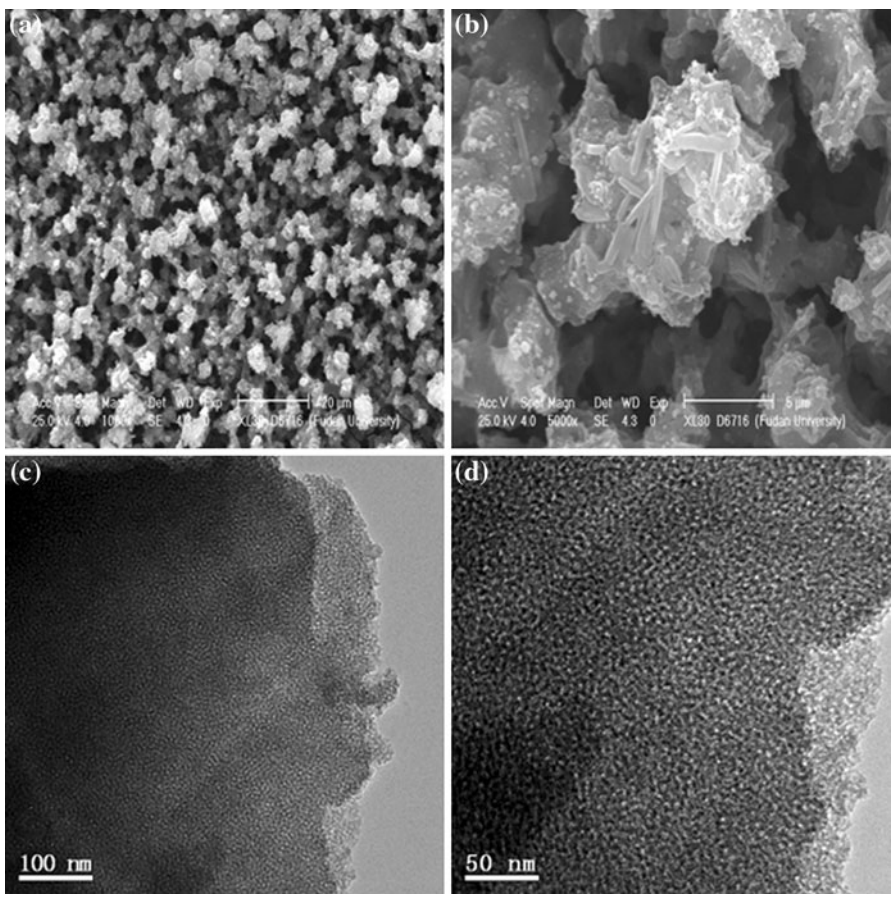

Fig. 4 **a**, **b** SEM images of adsorbent A. **c**, **d** TEM images of adsorbent A

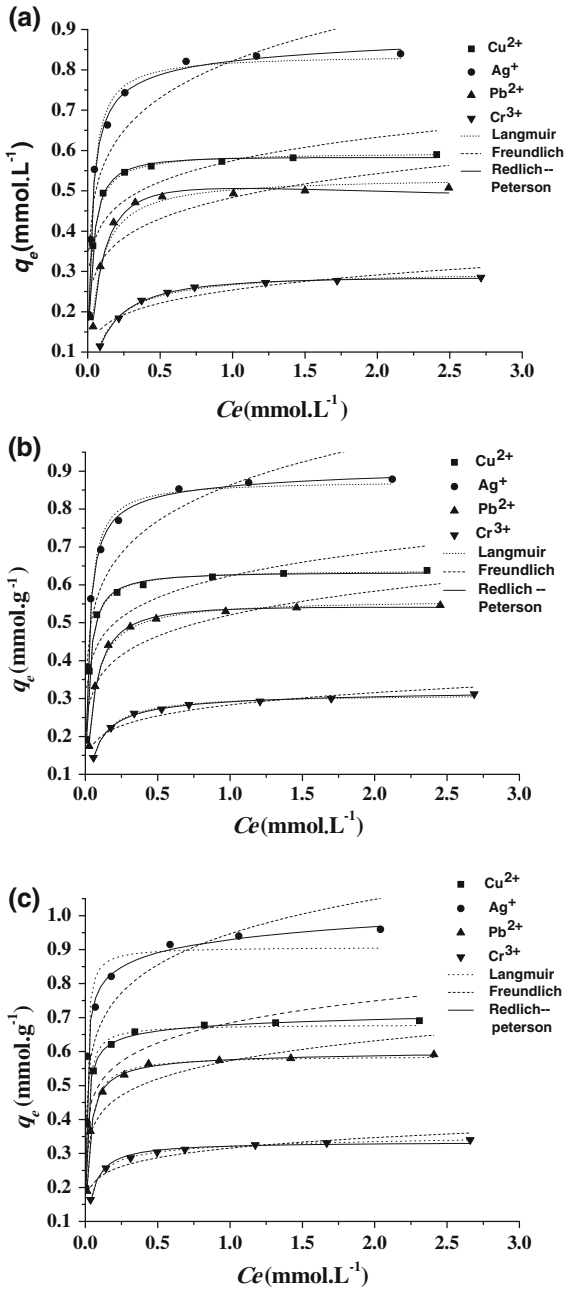

Fig. 5 Nonlinear fits of adsorption isotherm models for Cu(II), Pb(II), Ag(I), and Cr(III) adsorption on adsorbent A at **a** 293 K, **b** 303 K, and **c** 313 K

Xue and Li 2008). The SEM (Fig. 6a and b) and TEM (Fig. 6c and d) images of prepared adsorbent material (adsorbent A) and the same after trapping Cu(II) showed the possibility of heavy metal ions being reduced to metal nanoparticles within the pores after adsorption. It was clear that the pores of the adsorbent A were occupied by Cu(II). The adsorption equilibrium data of Cu(II) and Pb(II) ions were analyzed with the above Langmuir, Freundlich, and Redlich–Peterson adsorption equation. The adsorption data fit the Redlich–Peterson isotherm equation best, followed by the Langmuir isotherm. The β constant of the Redlich–Peterson isotherm equation was nearly equal to 1 (Xue and Li 2008; Quintelas et al. 2009) which indicates that the monolayer reaction of Cu^{2+}, Pb^{2+}, Ag^{+}, Cr^{3+} on adsorbent A was predominant, but it was not an ideal monolayer adsorption. The main adsorption process of the mesoporous adsorbents for heavy metal ions main is chemisorption. The basic assumption of the theory is that adsorption takes place at specific homogeneous sites within the adsorbent and once a metal ion occupied a reaction site, then no further adsorption occurred at that location.

In Fig. 5, it is clear that the equilibrium adsorption capacity of Cu^{2+}, Pb^{2+}, Ag^{+}, Cr^{3+} on adsorbent A was 38.12 mg g^{-1}, 66.04 mg g^{-1}, 92.08 mg g^{-1}, and 13.84 mg g^{-1} at 303 K, respectively. In the present study, the best adsorption capacity of thiol-MCM-41 material was 38.1 mg g^{-1} for Cu^{2+} ions. The hybrid materials showed different potential for copper adsorption: salicylaldehyde-SBA-15: 59.0 mg g^{-1} and SBA-15: 10.5 mg g^{-1} (Mureseanu et al. 2008); aminopropyl-MCM-41: 30.5 mg g^{-1} (Algarra et al. 2005); aminopropyl-MCM-41: 24.6 mg g^{-1} (Yang et al. 2008); mercaptopropyl-functionalized porous silica: 13.0 mg g^{-1} (Lee et al. 2001); EDTA modified SBA-15: 13.2 mg g^{-1} (Jiang et al. 2007); thiol-SBA-15: 36.4 mg g^{-1} (Xue and Li 2008). It can be observed that the adsorption efficiency of SH-MCM-41 is higher than that of most adsorbents. The remarkable characteristics of the thiol-functionalized mesoporous silicas material are the high surface area per unit mass and large number of mercapto groups, which may cause high adsorption capacity for metal ions. In Tables 3, 4, 5, it is clear that the equilibrium adsorption capacity for Cu^{2+}, Pb^{2+}, Ag^{+}, Cr^{3+} on adsorbent A decreased in the order: $Ag^{+} > Cu^{2+} > Pb^{2+} > Cr^{3+}$. The result was consistent with previous experimental results (Yang et al. 2008).

Table 6 showed the equilibrium adsorption capacity of Cu^{2+}, Pb^{2+}, Ag^{+}, Cr^{3+} on adsorbent A and adsorbent O. It was clear that the equilibrium adsorption capacity of heavy metal ions on functionalized mesoporous adsorbent was larger than non-functionalized mesoporous adsorbent. So, it was important method to

Table 3 Nonlinear fitting parameters and equations of the Redlich–Peterson model[a]

Temperature (K)	Heavy metal	Average value of fitting parameter				Equation
		P	α	β	r^2	
293	Ag^+	37.90	45.12	0.9691	0.9979	$q_e = 37.90Ce/(1 + 45.12Ce^{0.9691})$
	Cu^{2+}	22.67	38.09	1.003	0.9994	$q_e = 22.67Ce/(1 + 38.09Ce^{1.003})$
	Pb^{2+}	6.471	11.80	1.009	0.9988	$q_e = 6.471Ce/(1 + 11.80Ce^{1.009})$
	Cr^{3+}	2.006	6.456	1.014	0.9999	$q_e = 2.006Ce/(1 + 6.456Ce^{1.014})$
303	Ag^+	42.17	48.02	0.9790	0.9986	$q_e = 42.17Ce/(1 + 48.02Ce^{0.9790})$
	Cu^{2+}	29.63	46.33	1.005	0.9997	$q_e = 29.63Ce/(1 + 46.33Ce^{1.005})$
	Pb^{2+}	10.24	18.13	1.003	0.9991	$q_e = 10.24Ce/(1 + 18.13Ce^{1.003})$
	Cr^{3+}	5.160	16.70	0.9766	0.9999	$q_e = 5.160Ce/(1 + 16.70Ce^{0.9766})$
313	Ag^+	169.0	180.8	0.9455	0.9991	$q_e = 169.0Ce/(1 + 180.9Ce^{0.4550})$
	Cu^{2+}	72.98	106.6	0.9738	0.9984	$q_e = 72.98Ce/(1 + 106.6Ce^{0.9738})$
	Pb^{2+}	27.49	46.72	0.9868	0.9991	$q_e = 27.49Ce/(1 + 46.72Ce^{0.9868})$
	Cr^{3+}	10.49	31.68	0.9616	0.9995	$q_e = 10.49Ce/(1 + 31.68Ce^{0.9616})$

[a] pH = 5, weight of the adsorbent = 100 mg, sample volume = 100 ml, equilibration time = 60 min, oscillation frequency = 200 r min^{-1}

Table 4 Nonlinear fitting parameters and equations of the Langmuir model[a]

Temperature (K)	Heavy metal	Average value of fitting parameter				Equation
		b	Q	r^2	RL	
293	Ag^+	38.66	0.8379	0.9924	0.008548	$q_e = 32.39Ce/(1+38.66Ce)$
	Cu^{2+}	40.53	0.5954	0.9954	0.008157	$q_e = 24.13Ce/(1+40.53Ce)$
	Pb^{2+}	15.82	0.5342	0.9719	0.02064	$q_e = 8.451Ce/(1+15.82Ce)$
	Cr^{3+}	7.597	0.3021	0.9953	0.04203	$q_e = 2.295Ce/(1+7.597Ce)$
303	Ag^+	43.64	0.8755	0.9921	0.007580	$q_e = 38.21Ce/(1+43.64Ce)$
	Cu^{2+}	47.52	0.6398	0.9982	0.006966	$q_e = 30.40Ce/(1+47.52Ce)$
	Pb^{2+}	20.15	0.5617	0.9982	0.01627	$q_e = 11.32Ce/(1+20.15Ce)$
	Cr^{3+}	14.62	0.3124	0.9993	0.02229	$q_e = 4.567Ce/(1+14.62Ce)$
313	Ag^+	131.9	0.9077	0.9891	0.002521	$q_e = 119.7Ce/(1+131.9Ce)$
	Cu^{2+}	90.74	0.6795	0.9773	0.003660	$q_e = 61.66Ce/(1+90.74Ce)$
	Pb^{2+}	43.55	0.5880	0.9921	0.007596	$q_e = 25.61Ce/(1+43.55Ce)$
	Cr^{3+}	24.50	0.3347	0.9971	0.01342	$q_e = 8.200Ce/(1+24.50Ce)$

[a] pH = 5, weight of adsorbent A = 100 mg, sample volume = 100 ml, equilibration time = 60 min, oscillation frequency = 200 r min^{-1}

functionalize the mesoporous adsorbent with mercapto groups to improve the equilibrium adsorption capacity of heavy metal ions on adsorbent.

Effect of pH on adsorption

The effect of the solution pH on the adsorption of Cu^{2+}, Pb^{2+}, Ag^+, Cr^{3+} onto adsorbent A is shown in Fig. 7a. The Cu^{2+}, Pb^{2+}, Ag^+, Cr^{3+} removal efficiency increased as the solution pH increased from 2 to 5 and then remained constant with further increases in pH. This effect was mainly due to the protonation of the sulfur atom of the –SH group, which diminishes the ability of the –SH group to be involved in chelating Cu^{2+}, Pb^{2+}, Ag^+, Cr^{3+} from solution. When the pH was around 5, the heavy metals in solution existed in the forms $Pb(OH)^+$, $Cu(OH)^+$,$Cr(OH)^{2+}$ and $Cr(OH)_2^+$ (Yang et al. 2008; Xue and Li 2008; Wang et al. 2005), which favor adsorption. When pH is higher than 6, precipitation of metal hydroxides is expected (Wang

Table 5 Nonlinear fitting parameters and equations of Freundlich model[a]

Temperature (K)	Heavy metal	Average value of fitting parameter			Equation
		k	n	r^2	
293	Ag^{+}	0.8222	5.857	0.9083	$q_e = 0.8222Ce^{0.1707}$
	Cu^{2+}	0.5748	7.219	0.9283	$q_e = 0.5748Ce^{0.1385}$
	Pb^{2+}	0.4834	5.995	0.9487	$q_e = 0.4834Ce^{0.1668}$
	Cr^{3+}	0.2340	5.043	0.9764	$q_e = 0.2340Ce^{0.1983}$
303	Ag^{+}	0.8629	5.948	0.9001	$q_e = 0.8629Ce^{0.1681}$
	Cu^{2+}	0.6235	7.188	0.9067	$q_e = 0.6235Ce^{0.1391}$
	Pb^{2+}	0.5205	6.087	0.9127	$q_e = 0.5205Ce^{0.1643}$
	Cr^{3+}	0.2832	6.421	0.9388	$q_e = 0.2382Ce^{0.1557}$
313	Ag^{+}	0.9467	6.818	0.9113	$q_e = 0.9467Ce^{0.1467}$
	Cu^{2+}	0.6842	7.652	0.9003	$q_e = 0.6842Ce^{0.1307}$
	Pb^{2+}	0.5727	7.084	0.9207	$q_e = 0.5727Ce^{0.1412}$
	Cr^{3+}	0.3157	7.403	0.9521	$q_e = 0.3157Ce^{0.1351}$

[a] pH = 5, weight of the adsorbent = 100 mg, sample volume = 100 ml, equilibration time = 60 min, oscillation frequency = 200 r min^{-1}

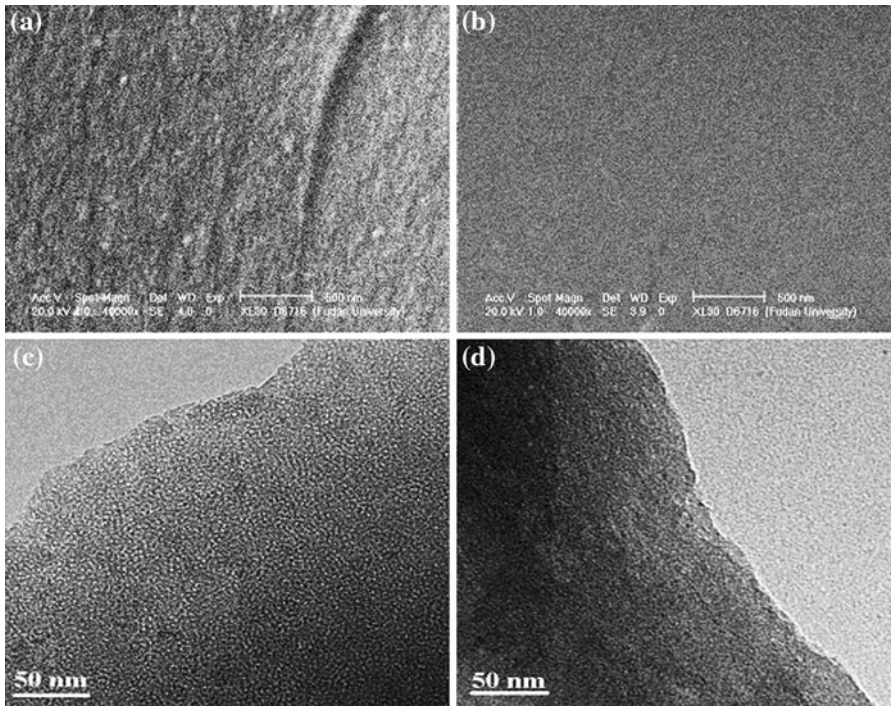

Fig. 6 **a**, **b** SEM images of adsorbent A and the same after trapping metal ions. **c**, **d** TEM images of adsorbent A and the same after trapping metal ions

et al. 2009; Bhattacharyya and Gupta 2007; O'Connell et al. 2006).

As shown in Fig. 7b, when adsorption process was complete the final solution pH was lower than the initial pH value. An exchange adsorption reaction between H^{+} of the –SH group in the framework of mesoporous materials and the heavy metal ions caused a general decline of the pH of the system. Figure 8 shows the adsorption mechanism of Cu^{2+} onto the adsorbent (Mureseanu et al. 2008). The mechanism for the removal of toxic heavy metal ions in an aqueous solution is the most either by electrostatic interaction

Table 6 The equilibrium adsorption capacity of Cu^{2+}, Pb^{2+}, Ag^{+}, Cr^{3+} on adsorbent A and adsorbent O[a]

Temperature (K)	Heavy metal	Equilibrium adsorption capacity/mmol L^{-1}	
		Adsorbent A	Adsorbent O
293	Ag^{+}	0.8273	0.1734
	Cu^{2+}	0.5564	0.1647
	Pb^{2+}	0.4931	0.1613
	Cr^{3+}	0.2673	0.1627
303	Ag^{+}	0.8774	0.1873
	Cu^{2+}	0.6123	0.1815
	Pb^{2+}	0.5137	0.1784
	Cr^{3+}	0.2839	0.1779
313	Ag^{+}	0.9237	0.1913
	Cu^{2+}	0.6673	0.1874
	Pb^{2+}	0.5724	0.1856
	Cr^{3+}	0.3119	0.1841

[a] pH = 5, weight of the adsorbent = 100 mg, sample volume = 100 ml, equilibration time = 60 min, oscillation frequency = 200 r min^{-1}

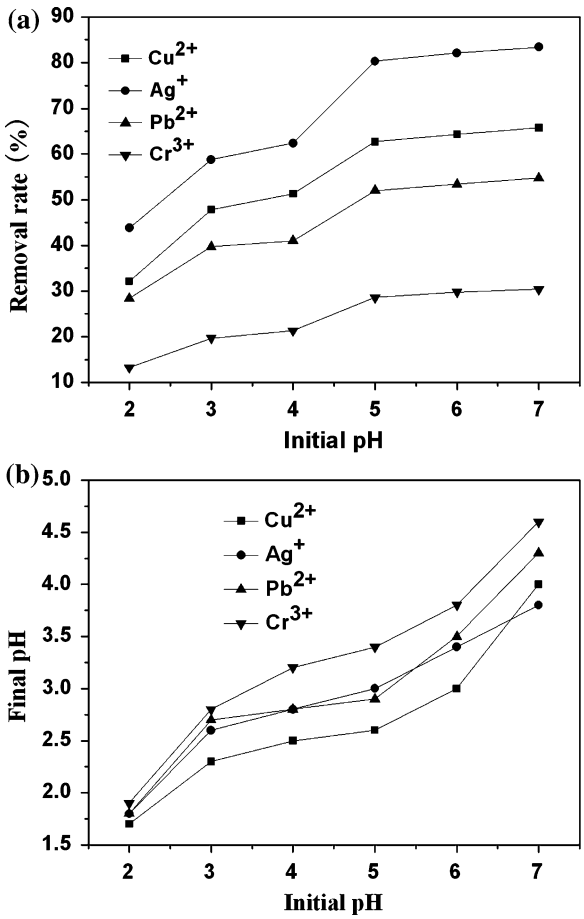

Fig. 7 **a** Effect of pH on adsorption for adsorbent A. **b** Comparison of the final and initial pH values

(ionic interaction between positively charged metal ions and negatively charged matrices) or by chelation (donation of the lone-pair electrons of the matrices to metal ions to form co-ordinate bonds) (Cestari et al. 2009; Quintanilla et al. 2006).

The optimum pH value for the removal of Cu^{2+}, Pb^{2+}, Ag^{+}, Cr^{3+} from solution ranged from 5 to 6. In this pH range, neither precipitation of the metal hydroxide nor protonation of the sulfur atom on the –SH group occurred.

Competitive adsorption on the functionalized mesoporous silica

A selectivity coefficient ($\alpha_{x/y}$) for the binding of heavy metal ion x in the presence of heavy metal ion y can be calculated according to Eq. 8:

$$\alpha_{x/y} = q_x c_y / q_y c_x \quad (8)$$

where q_x represents the equilibrium adsorption capacity of the adsorbent for heavy metal ion x, c_x is the equilibrium concentration (mmol L^{-1}) of heavy metal ion x in liquid-phase, q_y represents the equilibrium adsorption capacity of the adsorbent for heavy metal ion y, and c_y is the equilibrium concentration (mmol L^{-1}) of heavy metal ion y in liquid phase.

Table 7 summarizes the values for the equilibrium adsorption capacity (q_x, q_y), liquid-phase equilibrium concentration (c_x, c_y) and selectivity coefficients ($\alpha_{x/y}$) of adsorbent A for Cu^{2+}, Pb^{2+}, Ag^{2+}, Cr^{3+} in mixed

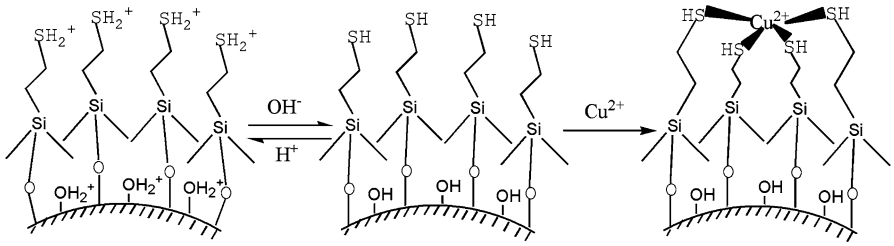

Fig. 8 The mechanism of adsorption of Cu^{2+} on the adsorbent

Table 7 Competitive adsorption on the functionalized mesoporous silica for Cu^{2+}, Pb^{2+}, Ag^{2+}, and Cr^{3+}[a]

Heavy metal		c_x (mmol L^{-1})	c_y (mmol L^{-1})	q_x (mmol g^{-1})	q_y (mmol g^{-1})	$\alpha_{x/y}$
x	y					
Cu^{2+}	Pb^{2+}	0.1060	0.4480	0.1831	0.1270	6.09
Ag^{+}	Cu^{2+}	0.0432	0.2251	0.1922	0.1531	6.57
Cu^{2+}	Cr^{3+}	0.0361	0.7432	0.1931	0.0813	49.2
Ag^{+}	Pb^{2+}	0.0460	0.4760	0.1923	0.1192	16.7
Pb^{2+}	Cr^{3+}	0.2133	0.7232	0.1570	0.0830	6.42
Ag^{+}	Cr^{3+}	0.0371	0.8461	0.1931	0.0741	59.6

[a] pH = 5, weight of the adsorbent = 100 mg, sample volume = 100 ml, equilibration time = 60 min, initial concentration of each heavy metal = 1.0 mmol L^{-1}, oscillation frequency = 200 r min^{-1}

solution. All the $\alpha_{x/y}$ values were greater than 6 and the adsorption capacities of Cu^{2+}, Pb^{2+}, Ag^{+}, Cr^{3+} have not decreased rather than solely adsorption, suggesting that the competing ions in the solution had little effect on the adsorption of Cu^{2+}, Pb^{2+}, Ag^{+}, Cr^{3+} by adsorbent A (Yang et al. 2008; Xue and Li 2008).

Effect of anions on adsorption

The effect of different anions (Cl^{-}, NO_3^{-}, SO_4^{2-}, CO_3^{2-}, OAc^{-} and Cit^{-}) on adsorption of Cu(II) is shown in Fig. 9. The adsorption was inhibited in the order: $NO_3^{-} < OAc^{-} < SO_4^{2-} < CO_3^{2-} < Cit^{-} < Cl^{-}$, depending on the coordination ability of the different anions. The presence of NO_3^{-} had little influence and the corresponding Cu(II) removal rate was 84.3%. The presence of Cl^{-} influenced the Cu(II) adsorption markedly, reducing the Cu(II) removal rate to 36.4%. Cl^{-} can react with Cu^{2+} to form stable complexes such as $CuCl_4^{2-}$, which have been observed previously by Barrow (Barrow and Cox 1992) in tests on metal oxides and soils.

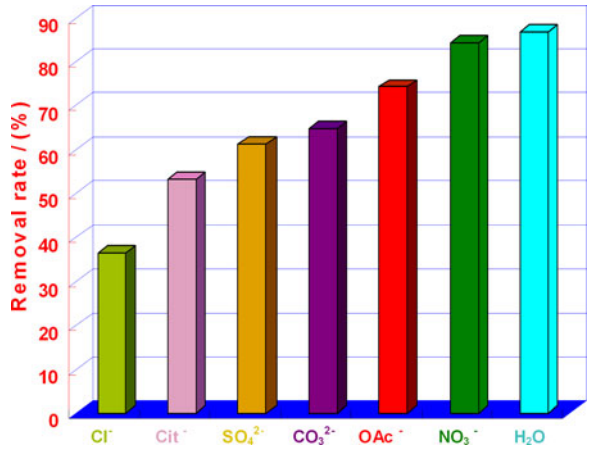

Fig. 9 Effect of anions on adsorption of Cu(II) by adsorbent A

Table 8 Effects of the regeneration process on adsorbent A[a]

Stripping cycle	Ag^+		Cu^{2+}		Pb^{2+}		Cr^{3+}		Sulfur content (wt%)
	q_e (mmol g^{-1})	Removal rate (%)	q_e (mmol g^{-1})	Removal rate (%)	q_e (mmol g^{-1})	Removal rate (%)	q_e (mmol g^{-1})	Removal rate (%)	
0	0.9151	91.5	0.6327	63.3	0.5273	52.7	0.3163	31.6	8.42
1	0.9052	90.5	0.6237	62.4	0.5214	52.1	0.3079	30.8	8.31
2	0.8961	89.6	0.6154	61.5	0.5138	51.4	0.3021	30.2	8.22
3	0.8910	89.1	0.6083	60.8	0.5054	50.5	0.2983	29.8	8.14
4	0.8852	88.5	0.6002	60.0	0.5013	50.1	0.2914	29.1	8.01
5	0.8763	87.6	0.5923	59.2	0.4967	49.7	0.2873	28.7	7.92
6	0.8714	87.1	0.5917	59.2	0.4873	48.7	0.2837	28.4	7.83

[a] pH = 5, weight of the adsorbent = 100 mg, sample volume = 100 ml, equilibration time = 60 min, initial concentration of Ag^+ = 1.0 mmol L^{-1}, temperature 303 K, oscillation frequency = 200 r min^{-1}

Recycling of adsorbent A

The results for the recycling and regeneration of adsorbent A after adsorption of Cu^{2+}, Pb^{2+}, Ag^+, and Cr^{3+} are shown in Table 8. The stripping agent used in this experiment was 1 mol L^{-1} HNO_3. According to Table 8, adsorbent A still removed 87.1, 59.2, 48.7, and 28.4% of Cu^{2+}, Pb^{2+}, Ag^+, and Cr^{3+} from solution after six extraction cycles. There was a total sulfur loss of 0.59% after six extraction cycles compared to the original sulfur content of 8.42%. The Ag^+ content in the extracted mesoporous adsorbent sample was 0.044 mmol g^{-1} after six extraction cycles, indicating that some ligands were irreversibly complexed and could not be regenerated by the acid treatment even though some –SH groups were physically lost by acid cleavage (Xue and Li 2008; Soundiressane et al. 2007). However, the adsorbed amount of Cu^{2+}, Pb^{2+}, Ag^+, and Cr^{3+} was still over 0.871, 0.592, 0.487, and 0.284 mmol g^{-1} even for the sixth extraction, showing that the adsorption capacity for Cu^{2+}, Pb^{2+}, Ag^+, and Cr^{3+} ion was almost fully restored.

Conclusions

A thiol-functionalized MCM-41 mesoporous silica with high adsorption capacity for Cu(II), Pb(II), Ag(I), and Cr(III) ions was synthesized by controlling the molar ratio of TEOS/MPTMS. The optimum molar ratio of TEOS/MPTMS was 4. With further addition of MPTMS, the S_{BET}, pore size, pore volume, and uniformity increased. The optimum pH value for removal of heavy metal ions from aqueous solution by functionalized MCM-41 ranged from 5 to 6. The mechanism is proposed to involve adsorption through ligand exchange with the –SH group. The equilibrium adsorption capacities for Cu^{2+}, Pb^{2+}, Ag^+, Cr^{3+} on adsorbent A were in the order: $Ag^+ > Cu^{2+} > Pb^{2+} > Cr^{3+}$. The presence of anions influenced Cu(II) adsorption in the order $NO_3^- < OAc^- < SO_4^{2-} < CO_3^{2-} < Cit^- < Cl^-$. According to the r^2 values, the adsorption isotherm fit the Redlich–Peterson nonlinear model. The removal rate for heavy metal ions was high, and the adsorbent could be regenerated by acid treatment without significantly altering its properties.

Acknowledgments The authors acknowledge the financial support of Ministry of Science and Technology for the Water Special Funding Program, Fund No. 2008ZX07421-002. We thank Dr. Pamela Holt, Shandong University, for assistance in preparation of the English manuscript.

References

Algarra M, Jimenez MV, Rodriguez-Castellon E, Jimenez-Lopez A, Jimenez-Jimenez J (2005) Heavy metals removal from electroplating wastewater by aminopropyl-Si MCM-41. Chemosphere 59:779–786

Barrow NJ, Cox VC (1992) The effects of pH and chloride concentration on mercury sorption. I. By goethite. J Soil Sci 43:295–304

Bendahou K, Cherif L, Siffert S, Tidahy HL, Benaïssa H, A-boukaïs A (2008) The effect of the use of lanthanum-doped mesoporous SBA-15 on the performance of Pt/SBA-15 and Pd/SBA-15 catalysts for total oxidation of toluene. Appl Catal A 351:82–87

Bhattacharyya KG, Gupta SS (2007) Adsorption accumulation of Cd(II), Co(II), Cu(II), Pb(II), and Ni(II) from water on montmorillonite: influence of acid activation. J Colloid Interface Sci 310:411–424

Burleigh MC, Dai S, Hagaman EW, Lin JS (2001) Imprinted polysilsesquioxanes for the enhanced recognition of metal ions. Chem Mater 13:2537–2546

Cestari AR, Vieira EFS, Vieira GS, Costa LP, Tavares AMG, Loh W, Airoldi C (2009) The removal of reactive dyes from aqueous solutions using chemically modified mesoporous silica in the presence of anionic surfactant—the temperature dependence and a thermodynamic multivariate analysis. J Hazard Mater 161:307–316

Correa FG, Becerril JJ (2009) Chromium(VI) adsorption on boehmite. J Hazard Mater 162:1178–1184

Jiang Y, Gao Q, Yu H, Chen Y, Deng F (2007) Intensively competitive adsorption for heavy metal ions by PAMAM-SBA-15 and EDTA-PAMAM-SBA-15 inorganic-organic hybrid materials. Microporous Mesoporous Mater 103:316–324

Kang T, Park Y, Yi J (2004a) Adsorption of Pt^{2+} and Pd^{2+} using thiol-functionalized mesoporous silica. Ind Eng Chem Res 4:1478–1484

Kang T, Park Y, Yi J (2004b) Highly selective adsorption of Pt^{2+} and Pd^{2+} using thiol-functionalized mesoporous silica. Ind Eng Chem Res 43:1478–1484

Kubilay S, Gürkan R, Savran A, Sahan T (2007) Removal of Cu(II), Zn(II) and Co(II) ions from aqueous solutions by adsorption onto natural bentonite. Adsorption 13:41–51

Lee B, Kim Y, Lee H, Yi J (2001) Synthesis of functionalized porous silicas via templating method as heavy metal ion adsorbents: the introduction of surface hydrophylicity onto the surface of adsorbents. Microporous Mesoporous Mater 50:77–90

Li J, Qi T, Wang L, Liu C, Zhang Y (2007) Synthesis and characterization of imidazole-functionalized SBA-15 as an adsorbent of hexavalent chromium. Mater Lett 61:3197–3200

Liu D, Lei JH, Guo LP, Du XD, Zeng K (2009) Ordered thiol-functionalized mesoporous silica with macrostructure by true liquid crystal templating route. Microporous Mesoporous Mater 117:67–74

Lu YK, Yan XP (2004) An imprinted organic-inorganic hybrid sorbent for selective separation of cadmium from aqueous solution. Anal Chem 76:453–457

Mangrulkar PA, Kamble SP, Meshram J, Rayalu SS (2008) Adsorption of phenol and *o*-chlorophenol by mesoporous MCM-41. J Hazard Mater 160:414–421

Mureseanu M, Reiss A, Stefanescu I, David E, Parvulescu V, Renard G, Hulea V (2008) Modified SBA-15 mesoporous silica for heavy metal ions remediation. Chemosphere 73:1499–1504

Naik SP, Fan W, Yokoi T, Okubo T (2006) Synthesis of a three-dimensional cubic mesoporous silica monolith employing an organic additive through an evaporation-induced self-assembly process. Langmuir 22:6391–6397

O'Connell DW, Birkinshaw C, O'Dwyer TF (2006) A chelating cellulose adsorbent for the removal of Cu(II) from aqueous solutions. J Appl Polym Sci 99:2888–2897

Quintanilla DP, Hierro ID, Fajardo M (2006) 2-Mercaptothiazoline modified mesoporous silica for mercury removal from aqueous media. J Hazard Mater 134:245–256

Quintelas C, Rocha Z, Silva B, Fonseca B, Figueiredo H, Tavares T (2009) Removal of Cd(II), Cr(VI), Fe(III) and Ni(II) from aqueous solutions by an *E. coli* biofilm supported on kaolin. Chem Eng J 149:319–324

Sayari A, Hamoudi S, Yang Y (2005) Applications of pore-expanded mesoporous silica. 1. Removal of heavy metal cations and organic pollutants from wastewater. Chem Mater 17:212–216

Soundiressane T, Selvakumar S, Ménage S, Hamelin O, Fontecave M, Singh AP (2007) Ru- and Fe-based N,N′-bis(2-pyridylmethyl)-N-methyl-(1S, 2S)-1,2-cyclohexanediamine complexes immobilised on mesoporous MCM-41: synthesis, characterization and catalytic applications. J Mol Catal A 270:132–143

Wang X, Lin KSK, Chan JCC, Cheng S (2005) Direct synthesis and catalytic applications of ordered large pore aminopropyl-functionalized SBA-15 mesoporous materials. J Phys Chem B 109:1763–1769

Wang JA, Zhou XL, Chen LF, Noreña LE, Yu GX, Li CL (2009) Hydroisomerization of n-heptane on the $Pt/H_3PW_{12}O_{40}$/Zr-MCM-41 catalysts. J Mol Catal A 299:68–76

Wei Q, Nie ZR, Hao YL, Chen ZX, Zou JX, Wang W (2005) Direct synthesis of thiol-ligands-functionalized SBA-15: effect of 3-mercaptopropyltrimethoxysilane concentration on pore structure. Mater Lett 59:3611–3615

Wu XW, Ma HW, Li JH, Zhang J, Li ZH (2007) The synthesis of mesoporous aluminosilicate using microcline for adsorption of mercury(II). J Colloid Interface Sci 15:555–561

Xue XM, Li FT (2008) Removal of Cu(II) from aqueous solution by adsorption onto functionalized SBA-16 mesoporous silica. Microporous Mesoporous Mater 116:116–122

Yang CM, Wang YQ, Zibrowius B, Schuth F (2004) Formation of cyanide-functionalized SBA-15 and its transformation to carboxylate-functionalized SBA-15. Chem Phys 6:2461–2467

Yang LM, Wang YJ, Luo GS, Dai YY (2005) Functionalization of SBA-15 mesoporous silica with thiol or sulfonic acid groups under the crystallization conditions. Microporous Mesoporous Mater 84:275–282

Yang J, Zhang J, Zhu LW, Chen SY, Zhang YM, Tang Y, Zhu YL, Li YW (2006) Synthesis of nano titania particles embedded in mesoporous SBA-15: characterization and photocatalytic activity. J Hazard Mater 137:952–958

Yang H, Xu R, Xue XM, Li FT, Li GT (2008) Hybrid surfactant-templated mesoporous silica formed in ethanol and its application for heavy metal removal. J Hazard Mater 152:690–698

Zhang L, Yu C, Zhao W, Chen H, Li L, Shi J (2007a) Preparation of multi-aminegrafted mesoporous silicas and their application to heavy metal ions adsorption. J Non-Cryst Solids 44–46:4055–4061

Zhang LX, Yu CC, Zhao WR, Hua ZL, Chen HR, Li L, Shi JL (2007b) Preparation of multi-amine-grafted mesoporous silicas and their application to heavy metal ions adsorption. J Non-Cryst Solids 353:4055–4061